Food Hydrocolloids Vol. 11 no. 4 pp. 373–384, 1997

Adhesion-strength characteristics of double-layered agar–galactomannan mixed gels

O.Ben-Zion and A.Nussinovitch[1]

The Hebrew University of Jerusalem, Institute of Biochemistry, Food Science and Nutrition, Faculty of Agricultural Food and Environmental Quality Sciences, PO Box 12, Rehovot 76100, Israel

[1]To whom correspondence should be addressed

Abstract

The adhesive-bond strength between adhered agar–galactomannan gel layers was determined, utilizing 90°-peel and tensile-bond tests. Five different independent variables were found to influence the adhesive strength between gel layers: gum concentration, type of galactomannan used, roughness of the layer interface, heat-maintaining capacities of the poured gel layers and the type of agar.

Introduction

The recent refinement and diversification of eating habits have brought about a demand for unusual and distinctive finished products, such as assembled jelly-type foods. Agar has commonly been used for such purposes, as has a sweetened curdlan-based multilayered gel (1–4).

Methods for preparing layered dessert gels have been previously published (5,6). They include pouring a hot hydrocolloid solution onto a pre-gelled layer, using hot melted hydrocolloid as a glue between already gelled layers, or simultaneously pouring hot hydrocolloid solutions. Mixed preparations of agar and galactomannans in multilayered gels have previously been reported (7).

Agar is a dried extract from different species of red algae. It is considered to be a complex mixture of two or three polysaccharides, all having the same backbone structure, but substituted to various degrees with charged groups. The important fraction, agarose, is the gelling component and is responsible for the gelling characteristics of agar gels. Agarose is essentially free of sulfate and consists of alternating chains of β-1,3-linked D-galactose and α-1,4-linked 3,6-anhydro-L-galactose (8). Its gelling mechanism relies specifically on the three equatorial hydrogen atoms on the 3,6-anhydro-L-galactose residues. These hydrogen atoms constrain the molecule to a helix and the interaction between these helices forms the three-dimensional agar gel structure (8). Galactomannans form a family of seed-reserve polysaccharides, based on a β-D-1,4-mannan backbone substituted with α-D-1,6-linked galactose stubs, which are present to varying degrees in different galactomannans (9). The tendency toward interchain associations decreases with increasing substitutions. The galactose substitutes, which are clustered in long blocks, are called the 'hairy regions', interspersed with regions of essentially non-substituted mannan backbone, called the 'smooth regions'. The least-substituted molecules exhibit the greatest tendency to associate within the galactomannan chain and with other polysaccharides (10).

The intermolecular mechanism of association between galactomannan and agar consists of the agar double helix binding to regions of the galactomannan backbone which are depleted in galactose residues. Locust bean gum (LBG), which has the lowest galactose content, provides the strongest interaction and guar gum the weakest, whereas tara gum is intermediate (11). The interactions between agar and galactomannans have been thoroughly investigated elsewhere (12,13). The supramolecular structure of such mixtures has recently been investigated by transmission electron microscopy (14). Much research has been undertaken on the intermolecular synergistic binding of xanthan and galactomannans (15–19) or kappa-carrageenan and galactomannans (20–22).

When layers consisting of other than gels are adhered to each other, the bond strength measured between layers is not an inherent property of the interaction. It also depends on the particular test method, the rate of loading, the thickness of the adhered layers, and other factors (23). The aim of this study was to check the adhesion between agar–galactomannan gel layers (chosen because they serve as a nice model

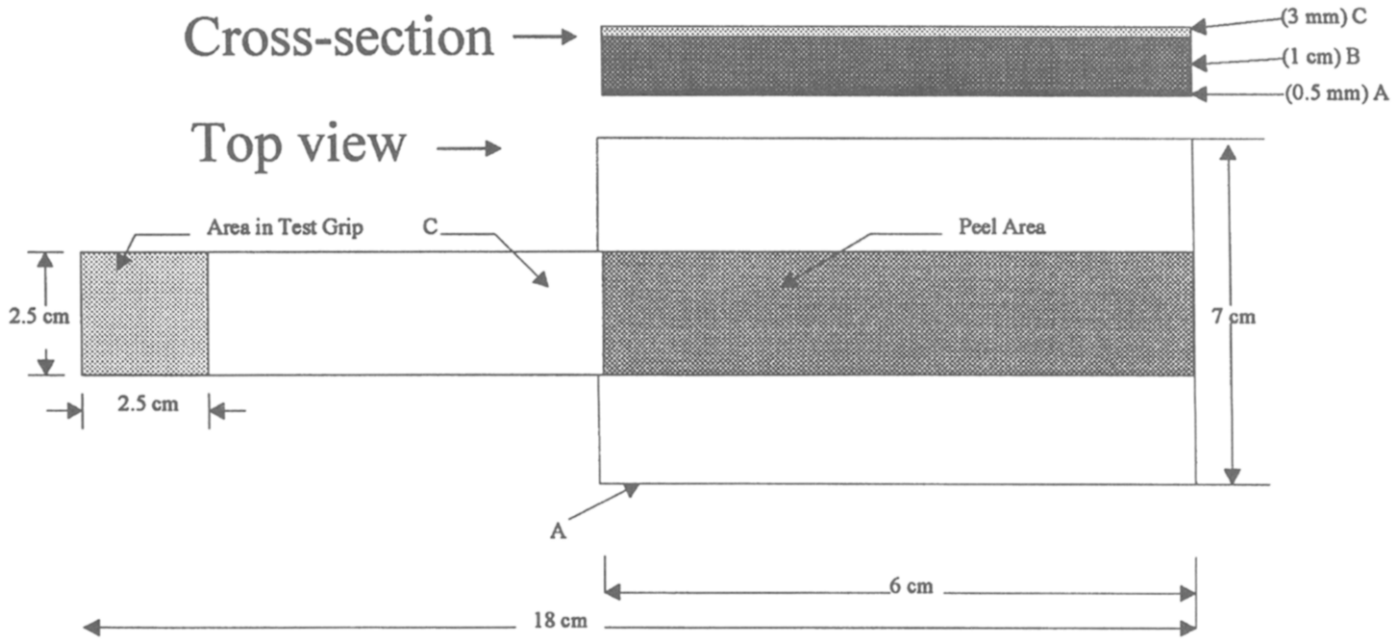

Figure 1 Schematic representation of the geometrical configuration of a specimen used for the 90°-peel test. A = rigid plastic; B = bottom layer gel; C = top layer gel.

for adhesion), to measure the forces involved in separating these layers, and to test whether the adhesiveness between component gel layers can be controlled.

Materials and methods

Sample preparation and mechanical tests

All the methods mentioned herein were chosen for a detailed study of the physical parameters related to the adhesion between agar–galactomannan gel layers. The sequence of the experiments was designed specifically to achieve this goal. Since previous studies have shown the possibility of building multilayered agar–galactomannan gels (5), it was logical to investigate the separation of such layers further by peeling and tensile tests. All peeling experiments were performed only with a special kind of agar which was chosen to enable folding of the layer at a 90° angle to the multilayered array. Once this obstacle had been overcome, we were able to study the influence of different concentrations of a variety of components on adhesion. Experiments were also conducted to verify the influence of roughness on peeling strength and adhesion.

Agar–galactomannan gel layers were glued together to form double-layered assemblies according to a previously described technique (5), whereby a hot solution of hydrocolloid or a hydrocolloid mixture is poured onto an already gelled layer of identical or different composition, at room temperature, to produce multilayered gels.

Gelidium japonicum agar extract (Matsuki Agar-Agar Industry Co., Chino-shi, Nagano-ken, Japan) was dissolved by mixing the powder in double-distilled water for 15 min and than heating the solution to 75°C. One of the following galactomannans, LBG, guar gum (Sigma Chemical Co., St Louis, MO, USA) or tara gum (Unipectin, Swiss), was then added to the hot solution and mixed vigorously for 30 min. The solution was then heated to ~100°C and immediately poured into a custom-made mold produced from PVC plates (15 × 21 × 3 cm, width × length × height). After setting (20°C for 1 h), the 3-mm-thick gel was used as the first (bottom) layer of the assembly. The gel layer was turned upside down to eliminate the occasional air bubble on its surface, and the second (upper) layer, of the same composition, was poured on top of the first to a thickness of 1 cm. The precise thicknesses of the gel layers were achieved by using a constant volume of liquid. Soon after pouring the upper-layer solution, the mold was sealed with a PVC top cover to decrease temperature loss to the environment and to keep the relative humidity at ~100% for 48 h before testing. The specimens were than cut from the molds in double-layered strips. The strips were turned such that the thicker, 1 cm layer was facing downward and glued with cyanoacrylate superglue (Allco, Osaka, Japan) to a rigid plastic, 0.5-mm-thick platelet (Fig. 1). Cyanoacrylate glue has previously been used to join cylindrical gels to a base plate in a tensile-bond test (24). The assembly, designed to be used in a 90°-peel test to determine the bond strength between agar–galactomannan mixed gel layers, was mounted on a special sliding rack to maintain a fixed angle during peeling (Figs 2 and 3). The jig [a device that holds a piece of work and guides the tools working on it (*The Oxford Paperback Dictionary*)] was designed to move the test panel at the same rate as the upper gel layer being stripped. It was connected to the bridge of an Instron Universal Testing Machine (UTM;

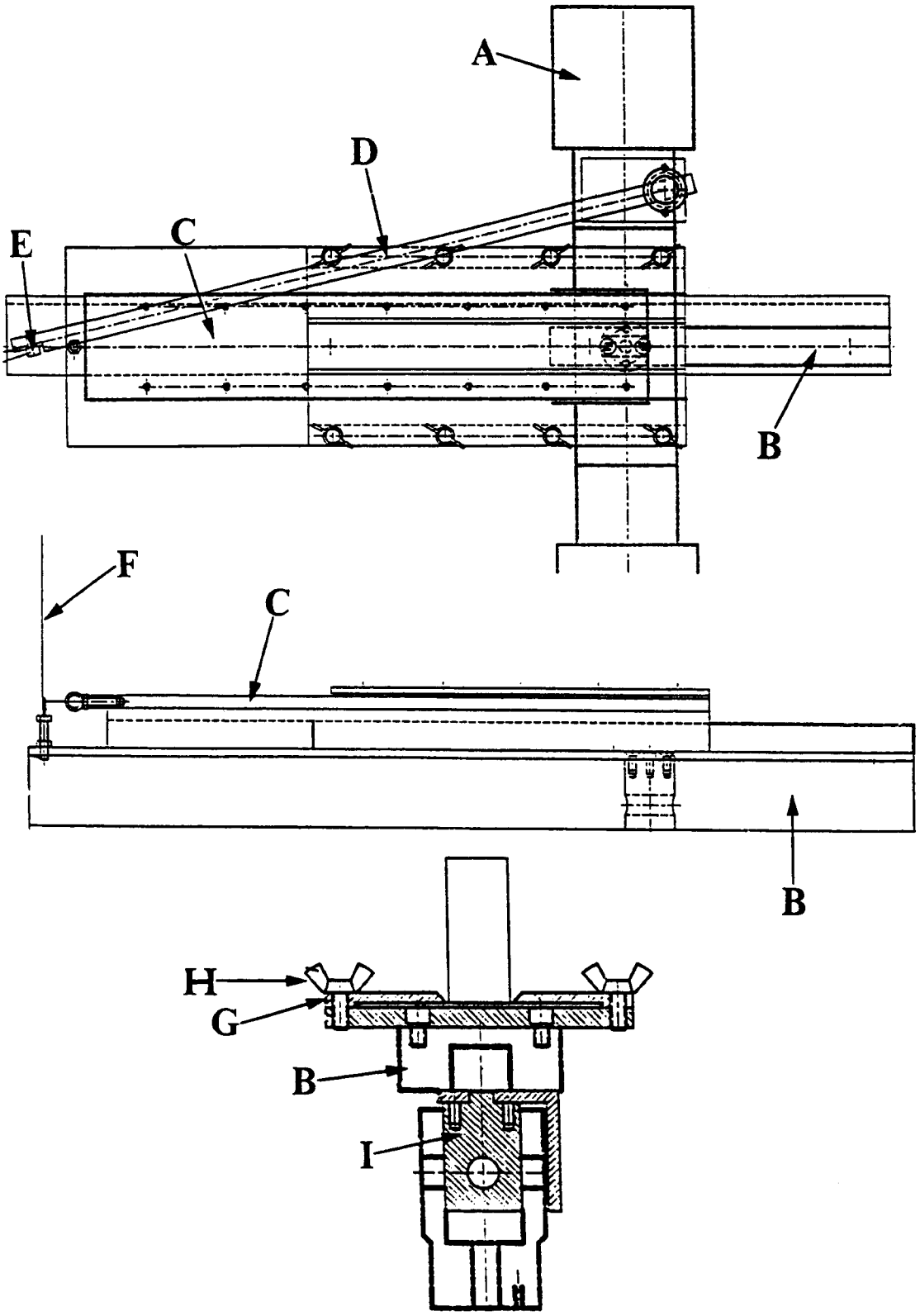

Figure 2 The geometry of the peeling accessory for the Instron UTM. Upper = top view; middle = side view; bottom = cross-section; A = UTM bridge; B = sliding rack; C = specimen base; D = lever; E = grip for wire; F = metal wire; G = clamp-plate; H = screw; I = fixture joint.

Instron Co., Canton, MA, USA, Model #1100) by a frictionless, 0.05-mm-diameter wire (Luma®, Sweden) (Fig. 3). The Instron was interfaced to an IBM-compatible computer with a card. A program bought from the Instron Company was used to perform data acquisition and to convert the UTM's continuous voltage versus time output

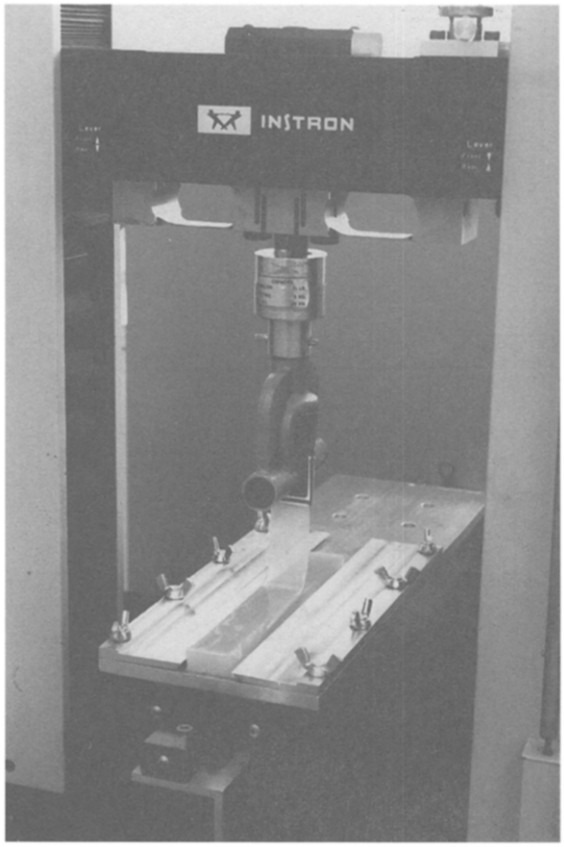

Figure 3 Specimen mounted on the Instron UTM during the 90° double-layered gel peel test.

into digitized force–deformation, force–time values with any desired definition of stress and strain. The upper gel strip was gripped at its upper edge to the Instron grip accessory and was wrapped in a Whatman® blotting paper (Whatman Int. Ltd, Kent), to prevent slippage. The *G.japonicum* agar extract was ideal for producing the gel layers to be peeled because of its inherent strength and elasticity.

All peel tests were performed at a cross-head speed of 200 mm/min along 3 cm (this speed was chosen after a few slower deformation rates had been tested). The mean peel-bond strength values were calculated as the force at debonding per unit width, considering only 2.25 cm (the first 7.5 mm were disregarded to achieve steady-state peeling conditions). Results represent an average of five specimens. Since the gel strip being peeled off the bottom-layer gel, mounted to the UTM grip, increases weight when debonding occurs, a calculation was performed to evaluate the 'real' bond force at a steady-state condition.

Preliminary gum concentration evaluation

Different variables were changed to achieve various compositional and physical properties of the double-layered gels. Five concentrations of LBG solution, 0.0, 0.2, 0.4, 0.6 and 0.8% (w/w), were added to four concentrations of agar solution (1.5, 2.5, 3.5 and 4.5%; w/w), yielding 20 mixed gel combinations to study the influence of concentration on peel-bond strength.

Roughness and adhesion determinations

The effects of gum concentration, type of galactomannan used and roughness of the bottom gel layer on peel-bond strength were studied by constructing gels with the four different agar concentrations (1.5, 2.5, 3.5 and 4.5%), combined with a constant galactomannan (LBG or tara gum or guar gum) concentration of 0.4%. Each hot agar–galactomannan solution was poured onto a polished PVC surface or onto one of four screens with different roughnesses to yield the bottom layer of the combined gel. The screens had the following characteristics: width (w) = 1.0 mm, depth (d) = 0.56 mm; (w) = 0.5 mm, (d) = 0.32 mm (Fig. 4A.I); (w) = 0.2 mm, (d) = 0.14 mm; and (w) 0.16 mm, (d) = 0.112 mm (Fig. 4B.I), respectively (Kurt Retsch GmbH & Co., Haan, Germany). After setting for 1 h, the rough gel layers (Fig. 4A.II and B.II) were removed from the screens and transferred to the standard sealable PVC molds with their rough surfaces facing upward. The second, identical, upper-layer hot solution was then poured to produce double-layered gels, as described above. All screens were scrupulously cleaned after each gel's removal in an ultrasonic apparatus (Bandelin Electronics, Berlin, Germany) for 15 min at ~100°C before re-use. Peel tests using the screen-produced surfaces were performed in one direction (see arrow in Fig. 4A.I and B.I). In addition, another experiment using rough plastic mold (Fig. 5) was performed. Coloring, β-carotene (Sigma), was included in the bottom layer to enhance the visual contrast between layers, before photographing the gel assembly.

The friction constants of two mixed gel layers of identical composition [3.5% (w/w) agar (*G.japonicum* extract) and 0.4% (w/w) LBG] and different roughnesses (as achieved by the aforementioned screens) were estimated by standard friction test (Fig. 6) at a constant speed of 20 mm/min with the sliding platform moving in the direction of the arrows in Figure 4A.I and B.I. Each test was repeated six times. The apparatus, which was specially designed for this purpose, is shown in Figure 7.

Relationship of peel-bond strength to melting temperatures

The effect of different agar types and heating temperatures on tensile-bond strength was studied by using 5% (w/w) agar of three different types: *G.japonicum* extract, agarose and purified agar (the latter two from Sigma). The three agars were dissolved by mixing the powder into double-distilled water for 15 min and heating the solution to the different temperatures listed in Table 1. The solutions were poured into custom-made PVC molds to produce the first (bottom) layer of the gel, at a thickness of 1.5 cm. After setting and gelling at 20°C for 1 h, the second (upper) layer, of the same composition, was heated and than cooled to the temperatures listed in Table 1 and poured over the first layer

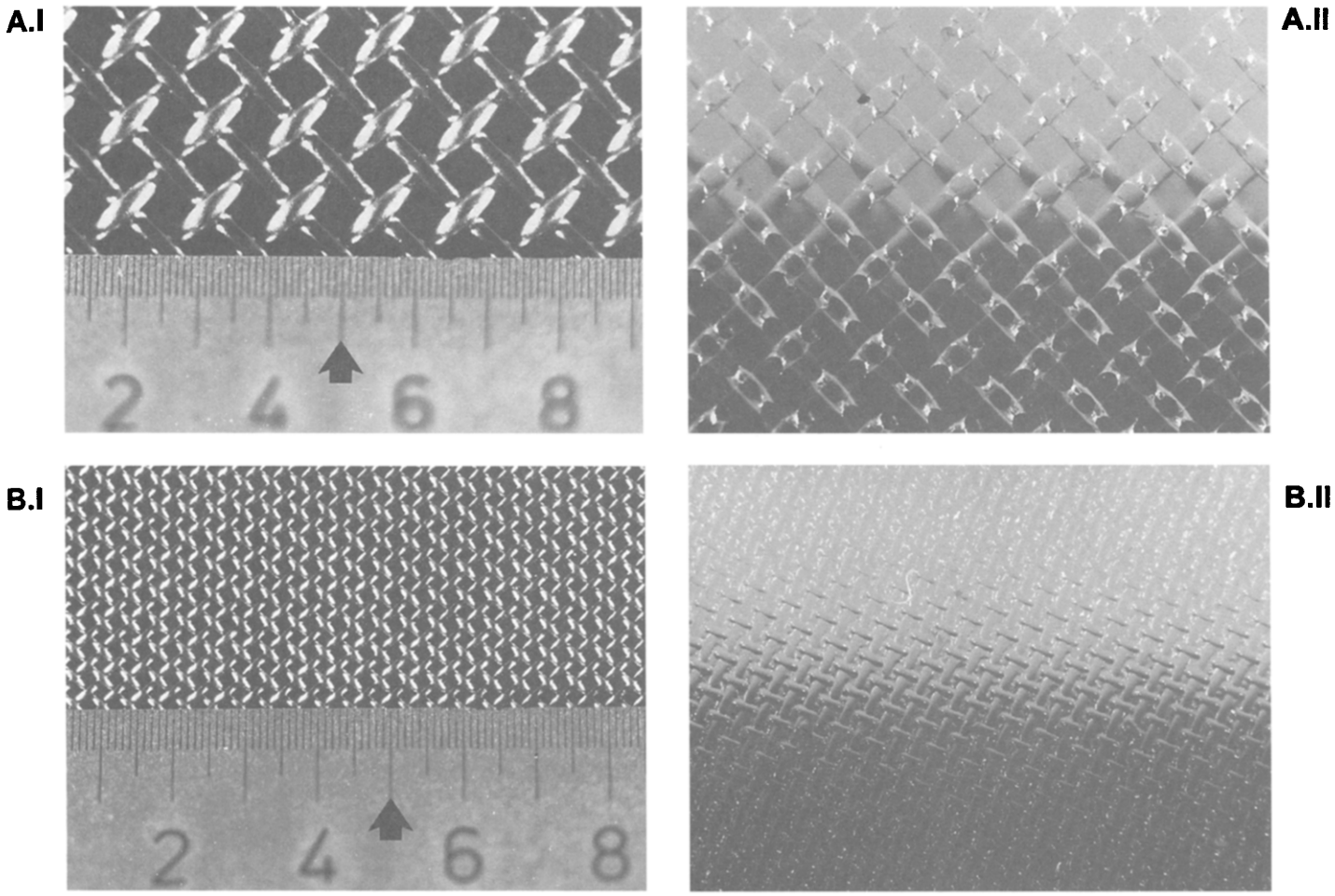

Figure 4 Two of the screen molds used for gel replication. (A.I) (w = 0.5 mm; d = 0.32 mm). (B.I) (w = 0.16 mm; d = 1.112 mm). Each scale

at a thickness of 1.5 cm. Soon after pouring the upper layer, the mold was sealed to eliminate evaporation and to decrease heat loss. After 48 h, specimens were cut to produce rectangular double-layered gels. These gels were attached on both sides to an equal-squared T-shaped PVC block, with cyanoacrylate superglue (Fig. 8). The blocks held by the UTM's grips were separated at a cross-head speed of 20 mm/min (Fig. 9A and B). Tensile-bond strength values were calculated as the force at debonding divided by the cross-sectional area of the interface.

Layer heat capacities

To check the influence of the heat-maintaining capacity of different volumes of pre-setting gel solutions, these were heated to 95°C and then poured and allowed to gel on top of a 3 mm agar–LBG gel layer. The assemblies were always turned upside down before peel tests were performed.

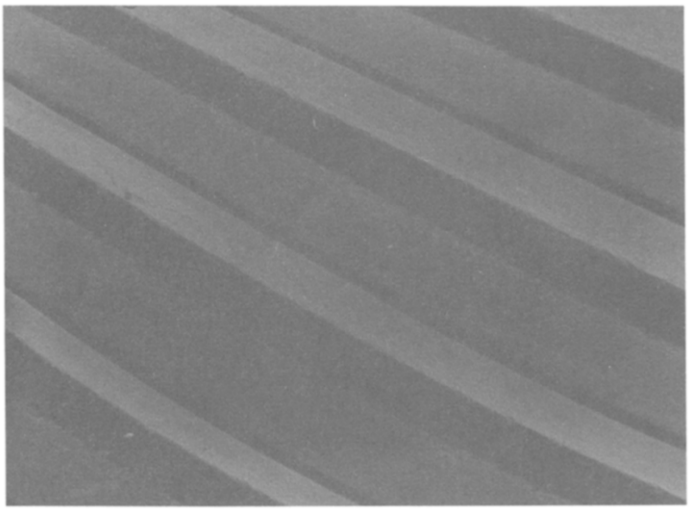

Figure 5 Truncated-triangle-shaped plastic used for making gel replicas (magnified ×15).

Theoretical methods

The magnitude of the frictional force F is given by Amonton's laws (25):

$$F = \mu_s N \quad (1)$$

$$F = \mu_k N \quad (2)$$

where N is the magnitude of the normal force, i.e. the perpendicular force with which each surface is pressed onto the other. The (dimensionless) coefficients μ_s and μ_k are the coefficients of static and kinetic friction, respectively. In a horizontal surface, $N = mg$, where g is the gravity constant and m is simply the sliding platform weight (a flexiglass platform with a total weight of 165 g), including the gel which is located at its central bottom surface (Fig. 7). Deviations from Amonton's laws (26,27) are frequently observed in practice. The deviations are especially marked because at $N = 0$ the friction force is not equal to zero. This leads to the following two-term formula expressing the dependence of the external friction force F on the normal load N:

$$F = \mu N + \mu AS \tag{3}$$

where μ is the 'true' friction coefficient, S is the area of true contact and A is the sticking force per cm^2 of the effective area of true contact S. The smallness of the second term in the above formula is a consequence of the smallness of the area of real contact (26,27). Since gels possess a wet-like surface, the term μAS may not be negligible because of an increase in A. To eliminate as completely as possible the appearance of considerable sticking forces during contact and deviations from Amonton's laws, the gels were blotted just before testing with a 12.5-cm-diameter Whatman® paper.

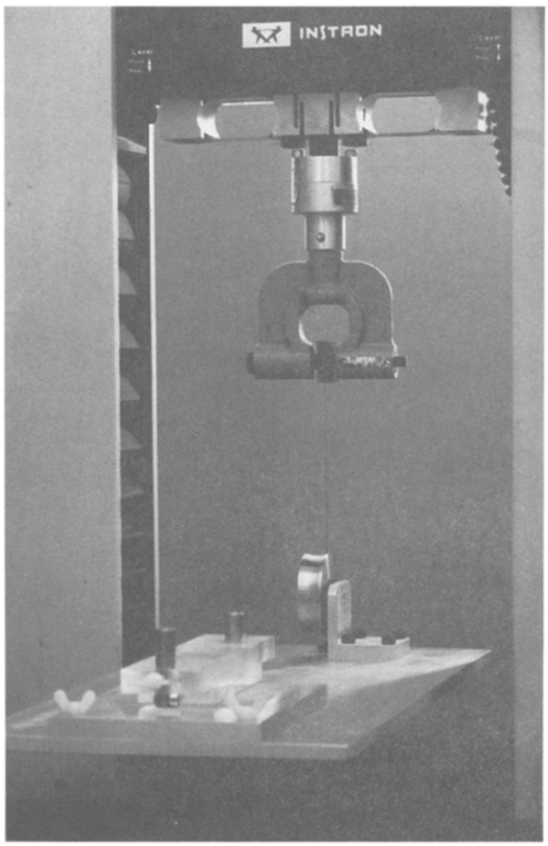

Figure 6 Specimen mounted on the Instron UTM during a standard friction test.

Results and discussion

To construct double-layered gel arrays, preliminary studies of different gum concentrations were performed. The highest 'practical' agar concentration for layer production was found to be not more than ~6.0%. Addition of as high as 0.8% (w/w) galactomannan to the gum mixture decreased the feasible agar concentration to not more than ~4.5%. It should be emphasized that in practice multilayered gel production makes use of very high viscosities at which the hot solution can be poured continuously into the molds. No such viscosity measurements were conducted here.

Typical curves for 90° gel–gel peeling are shown in Figure 10. The dashed line represents the calculated peel-bond strength. It is not surprising that whereas experimental results showed a small increase in peel-bond strength with

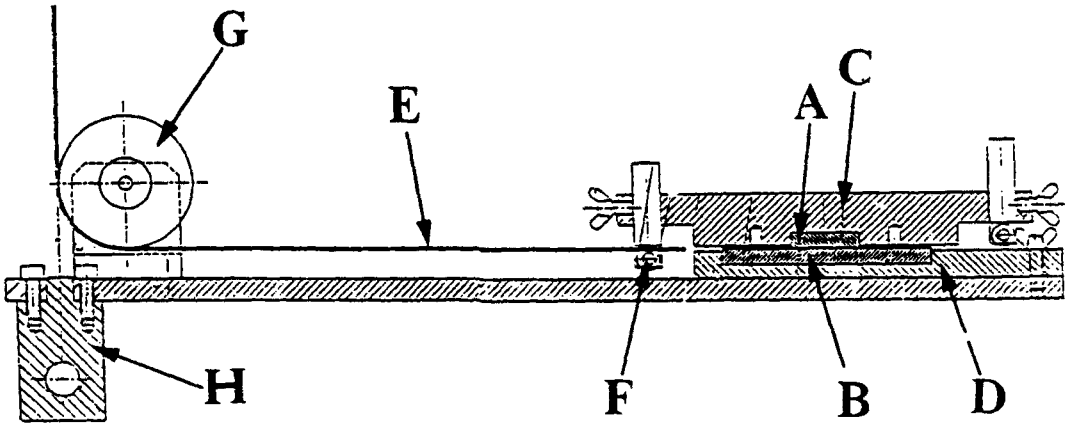

Figure 7 Side view of the friction accessory for the Instron UTM. A and B = gels; C = sliding platform; D = static platform; E = nylon string; F = grip; G = pulley wheel; H = fixture joint.

Table 1 Thermal properties and related parameters used to determine the relationship between the melting temperature of the bottom layer and bond strength

Agar type	Setting temperature[a] (°C)	Melting point[a] (°C)	Heating temperature (°C) (bottom layer)	Heating temperature (°C) (top layer)	Pouring temperature (°C) (top layer)
G.japonicum extract	43	95	95	100	100
				95	85
				95	75
Agarose	36	88	88	93	93
				88	78
				88	68
Purified agar	35	85	85	90	90
				85	75
				85	65

[a]Supplemented from the gum manufacturer.

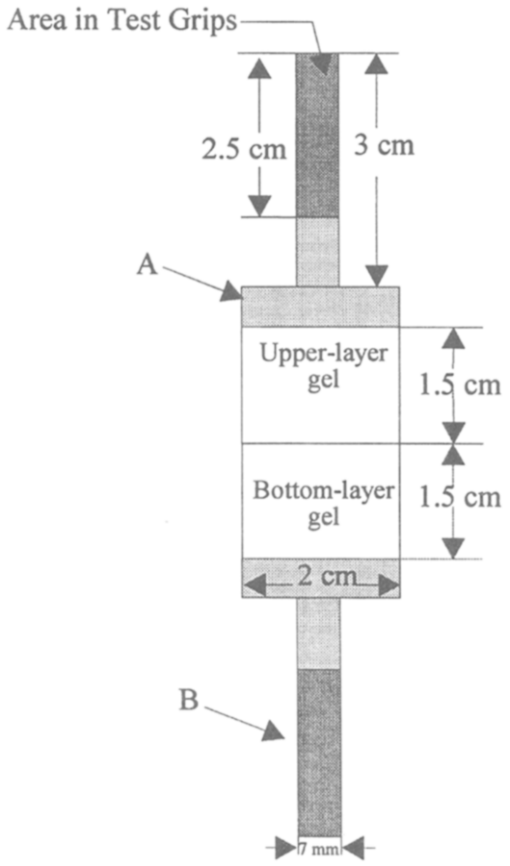

Figure 8 Cross-section of specimen geometry of double-layered gel used for tensile-bond test. A and B = PVC blocks.

time (or deformation), the theoretical (calculated) values are fairly rapidly constant after almost 3 s, reaching a pretty quick steady state.

The combined influence of agar and LBG concentrations on peel-bond strength is presented in Figure 11. It appears that an increase in agar concentration, and in LBG concentration up to 0.6%, increases the peel-bond strength. The presence of more then 0.6 and 0.8% LBG (which still contributed to the strength of the agar–LBG gel) seemed to cause a decrease in peel-bond strength. In the absence of LBG, the higher the agar gum concentration the higher the peel-bond strength. The mechanism of adhesion between these two identical layers could be explained as follows: when a hot agar or agar–galactomannan mixed gel is being poured onto another similar or identical already gelled layer and temperatures are higher than those which cause melting, then micro-melting of the 'bottom' monolayer at the interface can occur. Evidence of this phenomenon was observed in our study. Galactomannans differ from each other in their mannose:galactose ratio and in the distribution pattern of the galactose residues along the mannan chain. When reheating agar–galactomannan mixed gels above the melting point of the agar, the associations melt, eventually leaving unbound agarose helices (10). Those helices can interact with the galactomannan 'smooth regions' which will eventually be present in both layers. In other words, intermolecular interaction is suggested to be responsible for gel layer binding.

Figure 12A–C shows the influence of different bottom-gel roughnesses on peel-bond strength between identical gel layers. The concentration of the agar inside the layer was varied (1.5, 2.5, 3.5 and 4.5%), and was combined with a constant concentration (0.4%) of different galactomannans (LBG, tara gum or guar gum). A positive linear relationship between peel-bond strength and agar concentration (Fig. 12) was found regardless of the galactomannan used. At all three degrees of roughness, the peel-bond strength between agar–LBG double-layered gels was found to be higher than that between those including tara gum or guar gum. Possible intermolecular interactions could partially explain the changes in adhesive strength between double gel layers. In fact, the use of three galactomannans suggested that peeling strength is higher when the less substituted galactomannan was combined. However, the aim of our study was to measure physical properties related to adhesion and not to investigate fully the hypothetical intermolecular interactions which may be occurring.

It should be noted that the degree of substitution of the agar may also alter the interaction with the galactomannan.

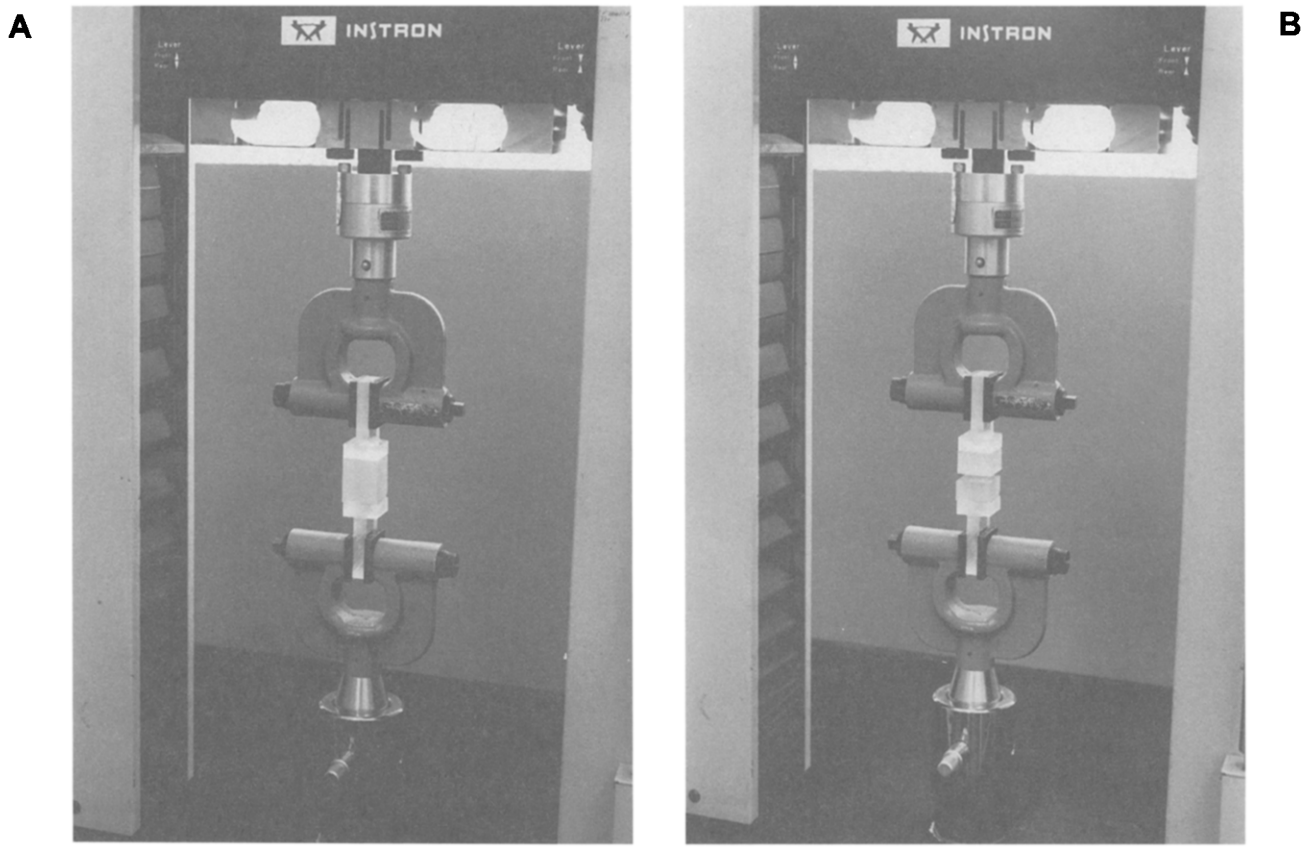

Figure 9 Specimen mounted on the Instron UTM (A) prior to application of tensile load and (B) after fracture.

Thus, the non-substituted agarose interacts much more strongly with a given galactomannan than the agar variants with increasing contents of methoxyl, sulfate and ketal groups (10). However, this observation goes far beyond the scope of this work.

The roughness degree of the bottom-layer surface significantly affected the strength of the bond between any two examined layers. Peel-bond strengths were directly dependent on the degree of roughness, decreasing with decreasing roughness (Fig. 12).

The screened and smooth surfaces of the molded gels were characterized by a friction test (see Materials and methods). In a curve of frictional force versus deformation (Fig. 13), two typical regions are observed: one where the force increases and decreases, and a second when the force reaches more or less constant values, i.e. static and kinetic, respectively. Although the transition from static to kinetic frictional force may seem abrupt, it is actually continuous.

The coefficients of friction were calculated based on equations (1) and (2) and are presented in Table 2. For a pre-determined surface, such coefficients are reasonably constant and theoretically independent of the contact area and, in the case of kinetic force, of the speed of the relative motion (25).

Both static and kinetic coefficients increased with the roughness of the screened gel, i.e. the smooth surface had the lowest static and kinetic friction coefficients and the surface with maximal roughness (w = 0.16 mm, d = 0.112 mm) resulted in the highest coefficients, whereas the surfaces with mid roughness (w = 0.2 mm, d = 0.14 mm; w = 0.5 mm, d = 0.32 mm; and w = 1 mm, d = 0.56 mm) yielded intermediate coefficients (Table 2).

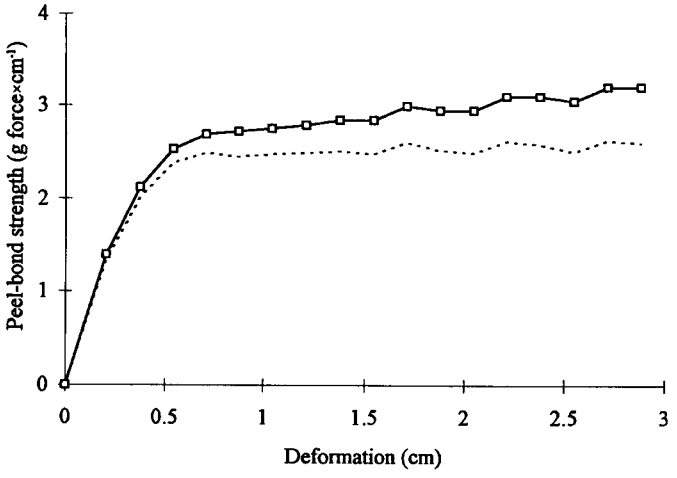

Figure 10 Typical curve for a double-layered gel (2.5% agar with 0.4% LBG) in a 90°-peel test. The dashed line represents the corrected peel-bond strength.

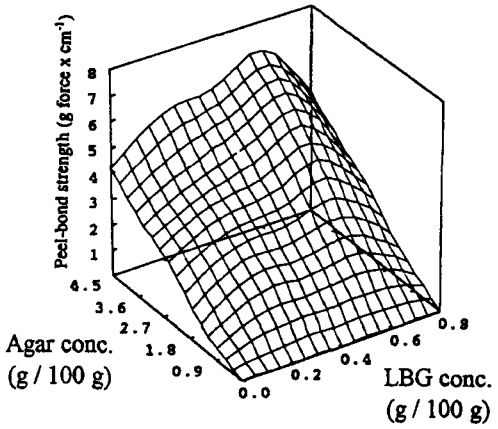

Figure 11 The effect of agar–LBG concentration on 90°-peel-bond strength of double-layered gels.

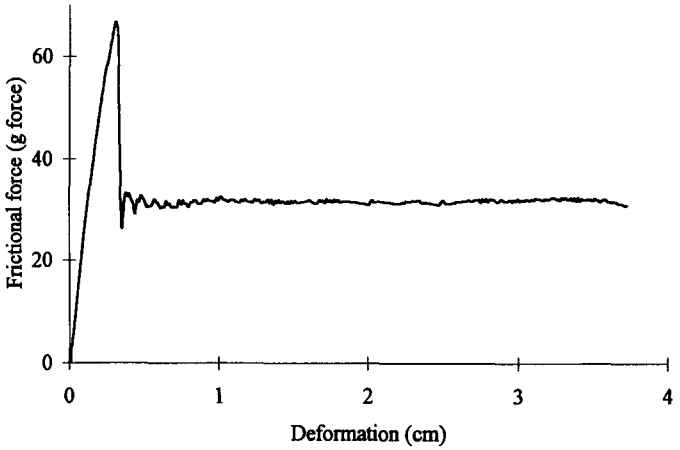

Figure 13 Typical curve of measured frictional force for identical bottom and top gels.

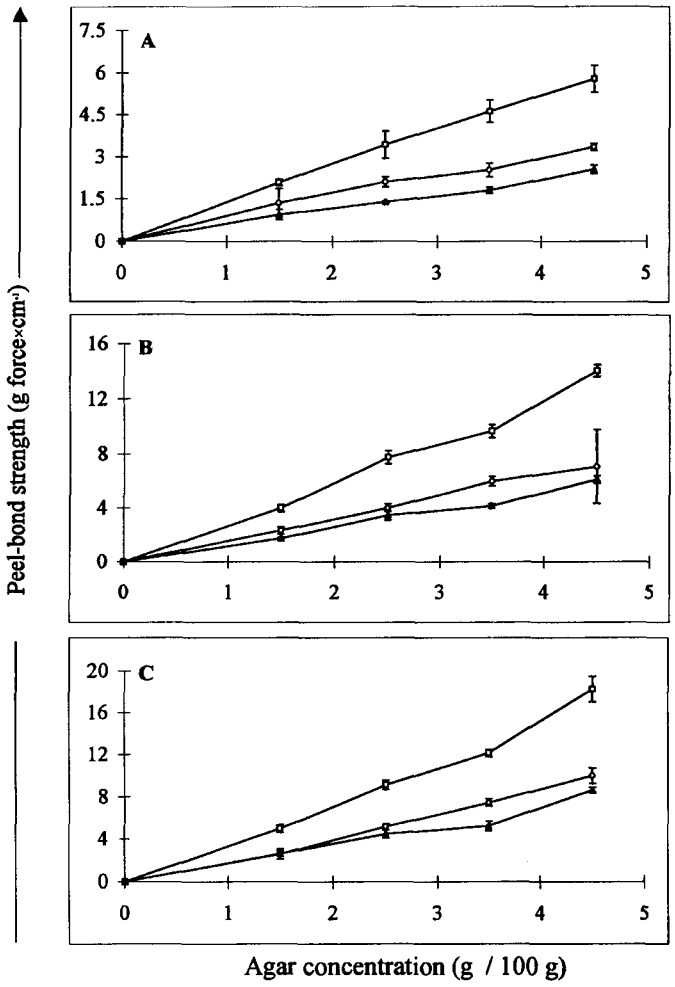

Figure 12 The influence of agar concentration, galactomannan type (□ = LBG; ○ = tara; △ = guar; all at a constant concentration of 0.4%) and the degree of roughness [(A) smooth surface; (B) w = 0.5 mm, d = 0.32 mm; (C) w = 0.16 mm, d = 1.112 mm] on the 90°-peel-bond strength of double-layered gels.

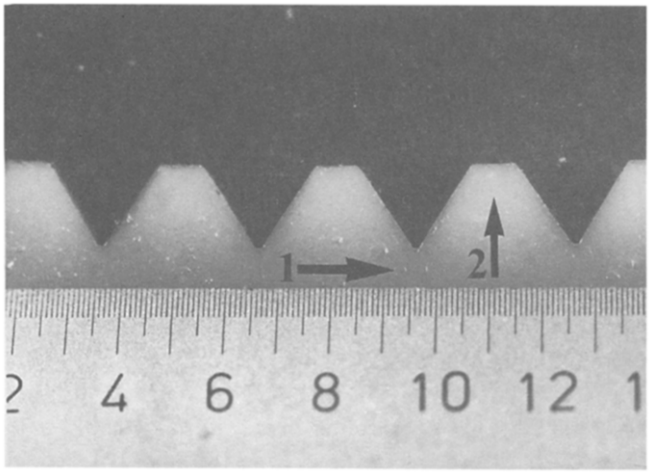

Figure 14 Double-layered gel with jagged layers. The light-colored bottom layer included β-carotene coloring to achieve visual phase separation. Each scale spacing represents 0.1 mm.

The mechanism governing the intermolecular interactions between gel layers depends on the surface of a given area. A higher contact area between gel layers is expected to yield an increase in measured peel-bond strength.

The degree of wetting is determined mainly by the viscosity and the surface tension of the pre-setting gel solution to be poured on top of the other gel, to create the double-layered system. The interfacial topography also plays a role via its influence on resistance to flow (28).

Pouring the upper layer at high temperatures (above the melting point of the agar) provides a relatively low viscosity which affects the contact angle of the liquid being poured and also the continuous melting of the bottom semisolid for a small period of time, sufficient to induce the process of bond formation.

After qualitatively checking the influence of interfacial roughness of the double-layered gel on peel-bond strength,

Table 2 Coefficients of friction obtained for the four screened and smooth gel replicas used in this study

Rougnness	μ_s	COV[a]	μ_k	COV
Smooth	0.13	7.69	0.05	12.00
Screened: w = 1.0 mm;d = 0.56 mm	0.14	6.25	0.06	6.28
Screened: w = 0.5 mm; d = 0.32 mm	0.23	5.65	0.12	5.00
Screened: w = 0.2 mm; d = 0.14 mm	0.29	7.38	0.14	7.35
Screened: w = 0.16 mm; d = 0.112 mm	0.39	1.03	0.18	7.22

[a]COV is the coefficient of variance, i.e. $100SD/\bar{X}$.

the quantitative contribution of this effect was evaluated using smooth versus rugged pre-determined surfaces (Fig. 5).

Figure 14 represents a cross-section of a double-layered gel produced using the mold, described in Materials and methods, where the bottom layer is whitish and the top layer black. The interfacial length was measured in the direction of the truncated triangles (Fig. 14, arrow 1) and found to be increased 1.56-fold over that of a smooth gel.

The mold used produced 10-mm-wide double-layered rough gel strips containing 3.5% agar combined with 0.4% LBG. In parallel, a smooth-surface double-layer strip of equivalent length (15.66 mm) was produced to study the influence of the glued surfaces (the contacting surface area) on adhesive strength. Peeling was performed as shown in Figure 14, arrow 2. The measured peeling bond strengths were compared by Student's *t*-test to verify their differences (five experiments per arrangement). No significant difference ($\alpha = 0.05$; $P = 0.29$) was found between the two values (7.78 versus 7.25 g force × cm^{-1}). These findings confirm that adhesion depends on the degree of roughness, i.e. the additional surface area it provides, and is independent of other factors involved. Finger joints used to produce long pieces of lumber or other wood constructions exploit this phenomenon. Generally, a rough surface is chosen to increase the adhesion between gel layers. In such a case, the shape and distribution of the bulges on the top of the gel should be considered. Such roughened gels, possessing increased surface area, can be used not only in foods, but for medical dressings and wound management, and for biotechnological immobilization applications.

Figure 15 exhibits the positive trend between achieved peel-bond strength and the respective coefficients of friction, μ_s and μ_k. Each point in this figure represents the average of five experiments, and five degrees of roughness. Strong linear relationships were calculated for both trends ($r = 0.92$ and 0.98 for the static and kinetic coefficients, respectively). The identical trends for both frictions verify the relationships between friction and adhesion, and justify the choice of the friction test to characterize the property of a potential gel to be adhered.

To test the role of the monolayer melting point at the

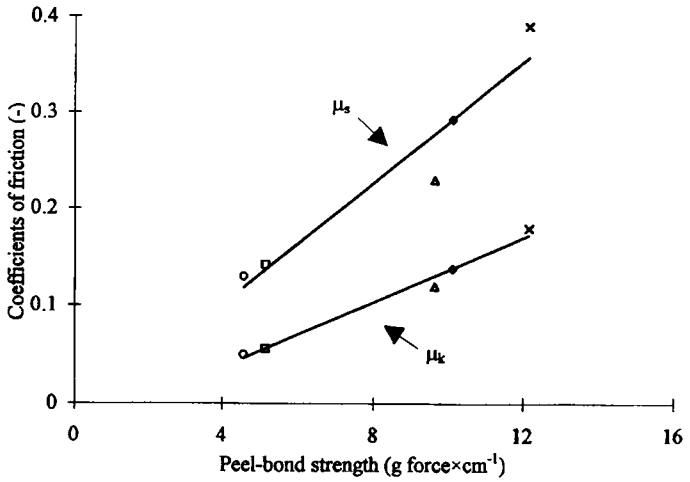

Figure 15 The correlation between coefficients of friction and peel-bond strength obtained for five roughnesses used in this work. ○, smooth surface; □, w = 1.00 mm, d = 0.56 mm; △, w = 0.5 mm, d = 0.32 mm; ◇, w = 0.2 mm, d = 0.14 mm; ×, w = 0.16 mm, d = 1.112 mm.

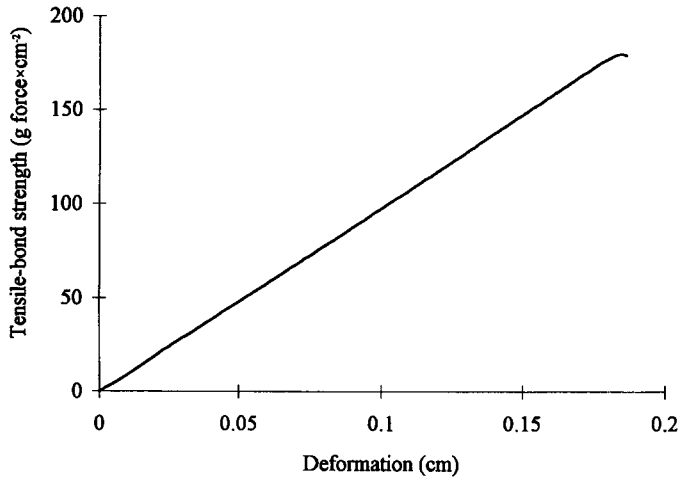

Figure 16 Typical tensile-bond curve for double-layered gels (agar from *G.japonicum* extract).

interface on the strength of adhesion between gel layers, three agar types having various melting points were chosen, and studied as described in Materials and methods.

Figure 16 represents a typical curve of tensile debonding to determine the strength of the adhesive bond between gel layers. The magnitude of the strain (deformation) at debonding depends on gel type, since no layer of adhesive is included between the two layers. This is similar to the technique of hot-melt adhesives, vulcanization, welding, polyethylene lamination to aluminum, etc., where the joint is often established at elevated temperature and pressure (23).

Figure 17 represents the tensile-bond strength obtained from the three agar types, each poured as a hot solution on their respective bottom layers. It should be noted that this is

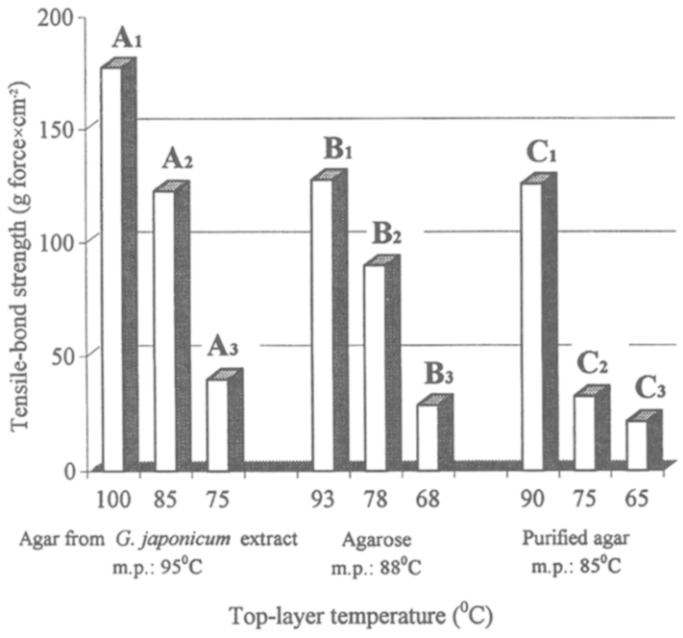

Figure 17 Tensile-bond strength for double-layered gels made with three different agar solutions cooled to various temperatures before molding onto an identical bottom-layer gel.

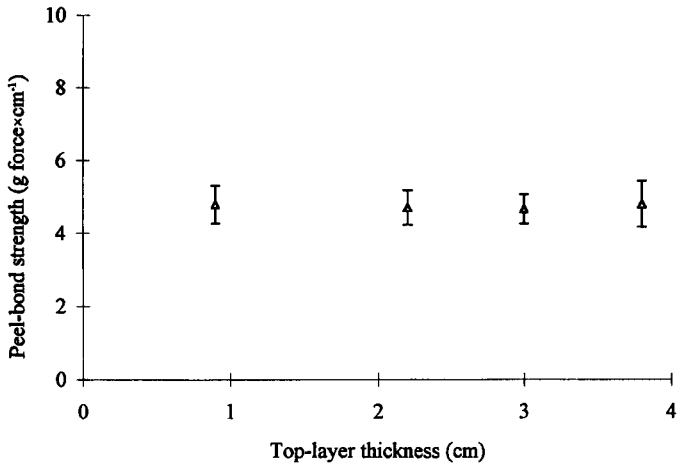

Figure 18 Relationships between top-layer thickness and 90°-peel-bond strength of double-layered gels made of agar and LBG.

the only test which can be used to measure bond strength since agars are generally brittle, except for *G.japonicum* extract. As can be seen from Table 1 and Figure 17, the upper hot solution was poured at 5°C above the melting point (m.p.) (columns A1, B1 and C1), 10°C below m.p. (columns A2, B2 and C2) and 20°C below m.p. (columns A3, B3 and C3), with A, B and C representing *G.japonicum,* agarose and purified agar, respectively. The ratios of A1 to A2 (1.44) and A2 to A3 (3.08) were more or less the same as those of B1 to B2 (1.42) and B2 to B3 (3.12), respectively. The ratios of C1 to C2 (3.86) and C2 to C3 (1.52) were different from the respective ratios of the other agar types used. These results indicate that at least for the *G.japonicum* extract and for the agarose, reducing the temperature at which the upper hot solution is poured results in a reduction in bond strength between vicinal layers. A top-layer solution whose temperature is equal to or above the melting point ensures even melting of the monolayer, and hence a well-bonded layer assembly.

In general terms, the kind of agar used to construct the gel layers significantly affects the adhesion pattern. Factors deriving from the molecular helical shape, degree of substitution and distribution of the chains may play a role in the intermolecular interactions.

Since the melting of the monolayer was considered a major factor influencing the layer's adhesion, different heat capacities of the poured layer were checked for influence on the peel-bond strength. Different volumes of pre-setting gel solutions at the same temperature (95°C) were used. The higher the volume of a particular solution, the better it maintains its high temperature. The peel-bond strengths of various top layers are presented in Figure 18. Statistical analysis (ANOVA, single factor) was performed to verify differences between the peeling strengths measured in this experiment. No significant statistical differences ($P = 0.97$, $\alpha = 0.05$) were found between the layers of different thicknesses in terms of their peel-bond strength. It is suggested that if the heat capacity of the poured layer is large enough to provide melting at the interface, resulting in molecular interactions, an increase in volume will not elevate the measured bond strength.

Conclusions

Double-layered gels made of different agar or mixed agar–galactomannan preparations were produced. The five studied factors—gum concentration, type of galactomannan, roughness of the interface, heat sensitivity of the layered gels and type of agar—had major effects on the adhesion between layers. Jelly-food-type preparations assembled according to the described methodologies can be produced as multilayered arrays, with excellent adhesiveness between participating gel layers. However, studies to evaluate the relationship between mechanical and adhesive properties and sensory evaluations are still needed.

Acknowledgements

We express our thanks to Dr Tetsu-jiro Matsuhashi, of Jiro Consulting Service to Food Technology and Seaweeds Utilization, Japan, for helping to provide a *Gelidium japonicum* agar extract, and to the Instrument Design Department of the Weizmann Institute of Science, Rehovot, Israel, who helped engineer peeling and friction accessories for the Instron Universal Testing Machine. The help of the photography experts O.Tevel, Z.Sadovasky and N.Bahat is greatly appreciated.

References

1. Harada,T. (1977) In Sanford,A. (ed.), *Extracellular Microbial Polysaccharides*. ASC Symposium Series, Washington DC, pp. 265–283.
2. Harada,T. (1979) In Blanshard J.M.V. (ed.), *Polysaccharides in Food*. Butterworths, London, p. 298.
3. Nussinovitch,A. (1997) *Hydrocolloid Applications, Gum Technology in the Food and Other Industries*. Blackie Academic & Professional, London, pp. 14–15, 229–246.
4. Nussinovitch,A., Lee,S.J., Kaletunc,G. and Peleg,M. (1991) *Biotechnol. Prog.*, **7**, 272–274.
5. Nussinovitch,A. and Ben-Zion,O. (1997) *Food Hydrocoll.*, **13**, 253–260.
6. Ohasi,S. and Iida,H. (1990) In Phillips,G.O. (ed.), *Gums and Stabilizers for the Food Industry 5*. IRL Press, Oxford, pp. 579–581.
7. Ben-Zion,O. and Nussinovitch,A. (1996) *Lebensm.-Wiss. Technol.*, **29**, 129–134.
8. Glicksman,M. (1979) In Blanshard,J.M.V. (ed.), *Polysaccharides in Food*. Butterworths, London, p. 190.
9. Smith,F. and Montgomry,R. (1959) *The Chemistry of Plant Gums and Mucilages*. Reinhold, New York, p. 324.
10. Dea,I.D.M. (1979) In Blanshard,J.M.V. (ed.), *Polysaccharides in Food*. Butterworths, London, p. 229–247.
11. Cairns,P., Morris,V.J., Miles,M.J. and Brownsey,G.J. (1986) *Food Hydrocoll.*, **1**, 89–93.
12. Gracia,R.B., Lopes,L. and Andrade,C.T. (1993) *Fresenius J. Anal. Chem.*, **344**, 510–513.
13. Turquois,T., Taravel,F.R. and Rochas,C. (1993) *Carbohydr. Polym.*, **238**, 27–38.
14. Gracia,R.B., DeBoinis,M. and Andrade,C.T. (1994) *Polym. Bull.*, 111–116.
15. Cairns,P., Miles,M.J. and Morris,V.J. (1986) *Nature*, **322**, 89–90.
16. Tako,M. (1991) *Carbohydr. Polym.*, **16**, 239–252.
17. Zhan,D.F., Ridout,M.J., Brownsey,G.J. and Morris,V.J. (1993) *Carbohydr. Polym.*, **21**, 53–58.
18. Fernandes,P.B. (1994) *Food Control*, **5**, 244–248.
19. Lundin,L. and Hermansson,A.M. (1995) *Carbohydr. Polym.*, **26**, 129–140.
20. Miles,M.J., Carroll,V. and Morris,V.J. (1984) *Macromolecules*, **17**, 2443–2445.
21. Cairns,P., Miles,M.J. and Morris,V.J. (1986) *Int. J. Biol. Macromol.*, **8**, 124–127.
22. Fernandes,P.B., Goncalves,M.P. and Doublier,J.L. (1991) *Carbohydr. Polym.*, **16**, 253–274.
23. DeVries,K.L. and Borgmeier,P.R. (1994) In Pizzi,A. (ed.), *Handbook of Adhesive Technology*. Marcel Dekker, NewYork, pp. 65–91.
24. Leliverre,J., Mirza,I. and Tang,J. (1992) *J Texture Stud.*, **23**, 349–358.
25. Halliday,D. and Resnick,R. (1988) *Fundamentals of Physics*. John Wiley & Sons, New York, pp. 104–107.
26. Dejaguin,B.V. and Toporov,Y.P. (1994) *Prog. Surface Sci.*, **45**, 308–316.
27. Dejaguin,B.V. and Toporov,Y.P. (1994) *Prog. Surface Sci.*, **45**, 317–327.
28. Gardon,J.L. (1966) In Patrick,R.L. (ed.), *Treatise on Adhesion and Adhesives*, Vol 1. Marcel Dekker, New York, pp. 286–323.
29. Cairns,P., Miles,M.J., Morris,V.J. and Brownsey,G.J. (1987) *Carbohydr. Res.*, **100**, 411.

Received on January 5, 1996; revised on May 23, 1996